

# Photodissociation of N<sub>2</sub>O<sub>4</sub> Multilayer Adsorbed on a Polycrystalline Au Substrate

Takehito Senga, Akihiro Yabushita, Yoshihiko Inoue, Masahiro Kawasaki\* and Shinri Sato†

Department of Molecular Engineering, Kyoto University, Kyoto 606-8501

†Catalysis Research Center and Graduate School of Environmental Earth Science, Hokkaido University, Sapporo 060-0811

(Received October 18, 2000)

The photodissociation dynamics of N<sub>2</sub>O<sub>4</sub> multilayers adsorbed on a polycrystalline Au substrate at 80–140 K was investigated. The Au substrate was mainly composed of domains with (111) structure. Time-of-flight spectra of the photofragment NO and O as well as infrared reflection absorption spectra for the surface adsorbed species on the Au substrate were measured. Typically, four to five monolayers of N<sub>2</sub>O<sub>4</sub> adsorb on the Au substrate at 85 K were irradiated by the pulsed output of an excimer laser at  $\lambda = 193$  and 351 nm. Photodissociation of the adlayers at 193 nm takes place by direct photoabsorption of N<sub>2</sub>O<sub>4</sub>. Since the top layers of N<sub>2</sub>O<sub>4</sub> absorbed the UV light, superthermal NO and O photofragments are produced. Translationally and internally relaxed fragments are also produced from the photodissociation of the inner layers. At 351 nm, the bulk photoexcitation results in formation of slow NO photofragments. By comparing the effect of dissociation wavelengths, substrate temperatures and dose rates, it is shown that the photodissociation dynamics is governed by both the photoexcitation process and the adsorption state of N<sub>2</sub>O<sub>4</sub> on the Au substrate.

Photodissociation of N<sub>2</sub>O<sub>4</sub> adsorbed on metal and insulator substrates is interesting as a typical system of inhomogeneous photoreactions. Dixon-Wallen et al.<sup>1</sup> reported the primary products and product internal states from the 248 nm photodissociation of N<sub>2</sub>O<sub>4</sub> physisorbed on single-crystal LiF (001) at 100 K. NO and NO<sub>2</sub> are the predominant products released into the gas phase, while some N<sub>2</sub>O<sub>3</sub> is probed on the surface. The product NO has a bimodal vibrational population in  $\nu = 0$ –9. The lowest vibrational level of NO( $\nu = 0$ ) corresponds to slowly moving photofragments. Hasselbrink et al.<sup>2</sup> reported the production of NO fragments from the photodissociation of a submonolayer of N<sub>2</sub>O<sub>4</sub> adsorbed on top of a NO saturated Pd surface at 193, 248 and 351 nm. They found two different desorption channels for NO: fast one and slow one. A polarization experiment with s- and p-polarized dissociation laser light indicates that the photodissociation channel is induced by metal excitation, that is,  $e^- + \text{N}_2\text{O}_4 \rightarrow \text{NO} + \text{NO}_3^-$ . A similar electron attachment process plays an important role in the 193 nm dissociation of N<sub>2</sub>O on Pd.<sup>3</sup> Sato et al.<sup>4</sup> investigated the adsorption states and the photodissociation mechanism of N<sub>2</sub>O<sub>4</sub> adlayers on Au(111) with mass spectroscopy and infrared reflection absorption spectroscopy (IRAS). They reported that N<sub>2</sub>O<sub>4</sub> physisorbed on Au(111) at a temperature < 120 K dissociates to NO<sub>2</sub> + NO + O at  $\lambda < 430$  nm. The NO desorbs from the surface, while part of the O atoms remain trapped on the Au substrate. NO<sub>3</sub> was not detected by IRAS on the surface during the photolysis. Since a thin water film on the Au inhibited the photodissociation yield of N<sub>2</sub>O<sub>4</sub>, it was suggested that the photolysis at  $\sim 350$  nm is enhanced by substrate photoexcitation via electron transfer from the substrate to the adsorbate. Crystalline N<sub>2</sub>O<sub>4</sub> multilayers are aligned preferentially

with the N-N axis perpendicular to an Au surface.<sup>4–7</sup>

Marsh et al.<sup>8</sup> reported the photodissociation of CH<sub>3</sub>Br on brominated Ni(111) at 193 and 248 nm. For high coverage of CH<sub>3</sub>Br on the Ni(111), fragmentation of CH<sub>3</sub>Br at 193 nm takes place primarily from the top layers of the adsorbates, with the underlying layers being caged and strongly inhibited. The onset of the velocity distributions of the fast photofragment is consistent with the expected gas-phase velocities, suggestive of direct photolysis of the top layers. These direct dissociation process was active up to 40 ML at 193 nm. The surface-mediated process occurs for a thin layer of CH<sub>3</sub>Br on the Ni(111) and slowly moving photofragments are produced. Similar results were reported for CH<sub>3</sub>I on iodided Cu(110) by Johnson et al.<sup>9</sup> and for C<sub>4</sub>H<sub>9</sub>ONO on Ag(111) by Jenniskens et al.<sup>10</sup>

In the present study we have investigated the photodissociation dynamics of N<sub>2</sub>O<sub>4</sub> adlayers on polycrystalline Au. Time-of-flight (TOF) and rovibronic spectra have been measured with the resonance-enhanced multiphoton ionization (REMPI) method for state-selected photofragments to elucidate dissociation dynamics. When we performed such an experiment at 248 nm, the observed results were in between the 193 and 351 nm cases. In this paper we report mostly the two extreme cases: direct dissociation at 193 nm and surface-mediated dissociation at 351 nm.

## Experimental

**A. Time-of-Flight Measurement of Photofragment NO at Kyoto.** Surface photodissociation on a cooled polycrystalline Au substrate was performed with a combination of a pulsed molecular beam, excimer laser and dye laser. The substrate is mainly com-

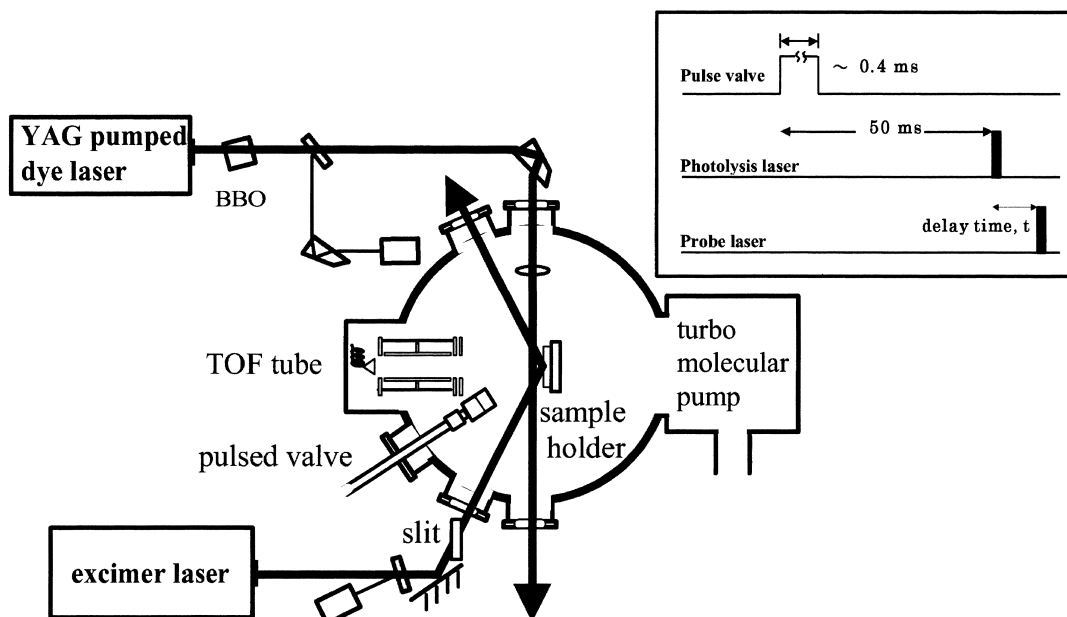


Fig. 1. Schematics of the experimental setup for resonance-enhanced multiphoton ionization (REMPI) detection of photofragments from the photodissociation of  $N_2O_4$  on a polycrystalline Au substrate at 193 and 351 nm. The time-of-flight spectrum is measured with a combination of pulsed molecular beam, excimer laser and dye laser. The inset shows the timing chart for molecular beam pulse, dissociation laser pulse, and probe laser pulse.

posed of domains with (111) structure. Our experimental setup is shown in Fig. 1. Neat  $NO_2$  was deposited on the Au substrate by expanding the gas with a pulsed molecular beam head (General Valve) every 100 ms, which was synchronized with dissociation laser triggers. The delay between molecular beam and photolysis laser triggers was typically set to 50 ms. The inset of Fig. 1 shows the timing chart for molecular beam, dissociation laser and probe laser pulses. Pulsed exposures of  $NO_2$  do not form a completely uniform layer of  $N_2O_4$  on the substrate during 50 ms annealing time below the desorption temperature. Since signal intensity did not depend on the delay for 10–90 ms, unwanted gas phase photodissociation was avoided and the photofragments from surface photodissociation were observed. By this intermittent dosing regime, the surface was almost replenished between the photodissociation laser shots. The intermittent dosing and REMPI detection regime was described by Masson et al.<sup>3</sup> A typical stagnation pressure of the gas valve was kept at 100 Torr (1 Torr = 133 Pa). In order to change effective exposures of  $NO_2$  on the substrate, the open gate time of the pulsed beam head was adjusted by changing the duration of the pulsed voltage to the head for 300–500  $\mu$ s. A vacuum chamber was pumped by two turbo molecular pumps in tandem (Seiko 600  $L s^{-1}$  and Mitsubishi 50  $L s^{-1}$ ). The chamber pressure was  $P = 0.5 \times 10^{-8}$  and  $1-10 \times 10^{-8}$  Torr without and with sample gas injection, respectively. The chamber pressure was monitored 50 cm away from the Au substrate with a cold cathode pressure gauge (MDC). Under these pressure conditions, a few monolayers of  $N_2O_4$  were formed on the substrate. The number of monolayers depends on the substrate temperature and the molecular beam pulse duration, which will be discussed below. The substrate temperature was controlled for  $T = 85-700$  K by a combination of conductive cooling with liq.  $N_2$  and resistive heating with an electric heater of a tantalum wire (0.33 mm dia.).

Polycrystalline Au substrates with (111) domains were prepared by DC glow-discharge sputtering, in which  $Ar^+$  bombard-

ment with low energy leads to atomic surface flatness of the sputtered films.<sup>11</sup> The substrate flatness was examined by scanning tunneling microscopy. The tilt angle was found to be at most  $5^\circ$ . This small tilt angle might cause an error within 1 % for calculation of the p- and s-polarization effect of the incident dissociation laser light. Typical grain sizes of the polycrystalline Au films were estimated to be submicrometers. The Au substrate was attached to a holder on a X–Y–Z stage in the vacuum chamber, which was cleaned by oxygen atoms produced from the 193 nm photodissociation of gaseous  $NO_2$  at  $T = 670$  K for 60 min. In this cleaning procedure, the excimer laser pulse was synchronized with the gas pulse of  $NO_2$ .

Probe pulse dye laser light (Lambda Physik, ScanMate, 0.2  $mJ cm^{-2} pulse^{-1}$ ) intersected the flux of NO and O. Those species were photodesorbed from the substrate upon irradiation of pulsed excimer laser light at 193 and 351 nm (Lambda Physik, COMPex, 10 Hz, 0.1–5  $mJ cm^{-2}$ ). TOF spectra were taken as a function of time delay,  $t$ , between photolysis and probe pulses. The time delay was controlled with a delay generator (Stanford Research). The one-photon transition of  $NO(A^2\Sigma - ^2\Pi_{3/2}, v'' = 0 \text{ and } 3, J'')$  was monitored by REMPI at 226 nm. The  $O(^3P_j, j = 0, 1, 2)$  atom was monitored by the two-photon resonant REMPI transition of  $O(^3D_j - ^3P_j)$  at 225.7–226.2 nm. The subsequent ion signals were detected with a homemade time-of-flight mass spectrometer (flight length = 25 cm).

For simulation of the TOF spectra, we first tested two different energy distribution functions, Gaussian and Maxwell–Boltzmann ones: fast photofragments correspond to a Gaussian distribution while slow ones correspond to a Maxwell–Boltzmann distribution.<sup>12–14</sup> However, it was found that a Gaussian distribution gives almost the same TOF distribution as a Maxwell–Boltzmann one when the translational temperature is around 600 K or less. Hence, for simplicity purposes, we used a composite of two Maxwell–Boltzmann distributions for a fast and a slow photofrag-

ments. In this simulation, it was assumed that a) photofragments are detected at a point REMPI detection region, b) photofragments come into the gas phase from a round substrate area (12 mm dia.) with a  $\cos^2\theta$  distribution where  $\theta$  is the departing polar angle from the substrate. The diameter of the effective substrate area was determined by a round slit in front of the chamber window for the dissociation laser, which is shown in Fig. 1 as a slit. The distance between the substrate and the detection region was changed from 3 to 5 mm. A typical distance was set to 3 mm. The assumption listed above was tested by the 351 nm photodissociation of  $\text{Cl}_2$  on Au. The observed TOF spectrum for the photoproduct Cl was well reproduced by the translational energy distributions reported by Giorgi et al.<sup>15</sup>

Unless otherwise noted, typical experimental conditions were  $P = 5 \times 10^{-8}$  Torr,  $T = 85$  K and  $1 \text{ mJ cm}^{-2} \text{ pulse}^{-1}$  at 193 nm and  $5 \text{ mJ cm}^{-2} \text{ pulse}^{-1}$  at 351 nm. This pressure condition corresponds to 4–5 ML of  $\text{N}_2\text{O}_4$  on Au, as will be discussed below.

**B. Infrared Absorption Measurement of Adsorbed Molecules on Surface at Hokkaido.** Infrared measurements were carried out in an ultrahigh vacuum chamber which has been described in detail previously.<sup>4</sup> An Au(111) single crystal (12 mm in diameter, 1.5 mm thick, 99.999% purity) substrate was cleaned by repeated Ar-ion sputtering at 800 K and was annealed at 900 K. Ozone was used for surface cleaning. After  $\text{NO}_2$  gas was deposited on the Au(111) by a pulsed molecular beam head, infrared reflection absorption spectroscopic (IRAS) measurements were performed. The IR beam from a FTIR spectrometer (BIO-RAD FTS-155) was p-polarized by a wire grid polarizer, and then was introduced into the vacuum chamber through a  $\text{BaF}_2$  window with the incident angle of the IR beam of  $85^\circ$ . IRA spectra were recorded with  $4 \text{ cm}^{-1}$  resolution and 200 scans. By measurement of IRAS absorption, the film thickness of  $\text{N}_2\text{O}_4$  was estimated to be about 4 ML on Au at 85 K in a dosing condition similar to Kyoto.

## Results

**A. Time-of-Flight Spectra of Photofragment NO and IR Spectra of Adsorbed  $\text{N}_2\text{O}_4$ .** Figure 2 shows typical TOF spectra  $S(t)$  of  $\text{NO}(X^2\Pi_{3/2}, v'' = 0, \text{Q-head})$  from the photodissociation at 193 and 351 nm as a function of time delay,  $t$ . The TOF spectra were simulated with a composite of flux-weighted Maxwell–Boltzmann translational energy distributions  $P(E_t)$  with a different translational temperature  $T_{\text{trans}}$ .  $P(E_t)$  is characterized by the average energy  $\langle E_t \rangle = 2k_B T_{\text{trans}}$ .<sup>16</sup>

$$S(t, r) = r^3 t^{-4} \exp\{-mr^2/(2k_B T_{\text{trans}} t^2)\}, \quad (1)$$

$$P(E_t) = (k_B T_{\text{trans}})^{-2} E_t \exp\{-E_t/(k_B T_{\text{trans}})\}, \quad (2)$$

where  $k_B$  is the Boltzmann constant and  $r$  is a flight length for photofragments. In the upper panel of Fig. 2 for 193 nm, a fast component **a** is characterized with  $T_{\text{trans}} = 600 \pm 30$  K and a slow one **b** with  $80 \pm 10$  K. The fast component **a** is dominant (80%) and the slow one **b** is minor (20%). In the lower panel for 351 nm, a fast component **a** is characterized with  $T_{\text{trans}} = 640 \pm 20$  K and a slow one **b** with  $80 \pm 10$  K. The slow component **b** is dominant (97%).

The inset of Fig. 2 shows the TOF spectrum of  $\text{NO}(X^2\Pi_{3/2}, v'' = 3, \text{Q-head})$  that was produced in the 193 nm photodissociation. The observed TOF spectrum for  $\text{NO}(v = 3)$  consists exclusively of the fast component **a** with  $T_{\text{trans}} = 635$  K. High

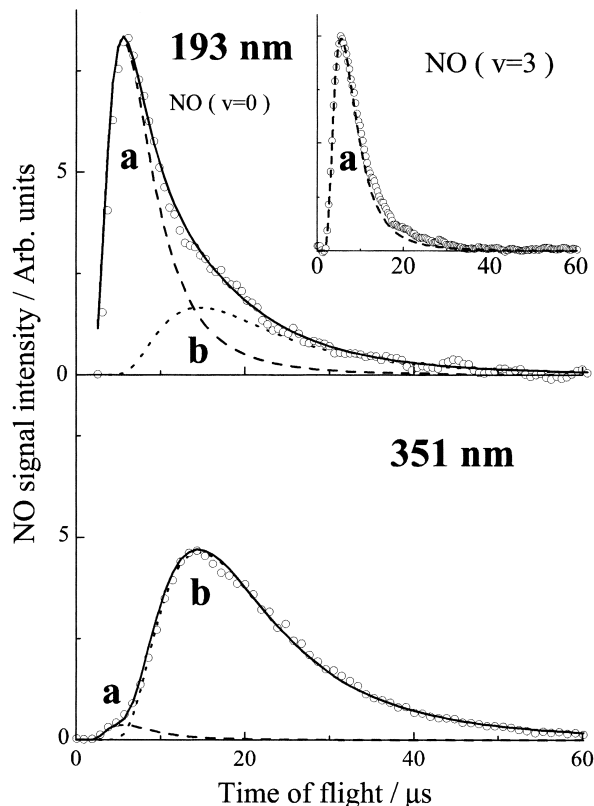


Fig. 2. REMPI time-of-flight (TOF) spectra of  $\text{NO}(X^2\Pi_{3/2}, v = 0, \text{Q-head})$  from the photodissociation of  $\text{N}_2\text{O}_4$  on Au at 193 and 351 nm as a function of delay time between dissociation and probe laser pulses. Circles are experimental results. The solid curve marked with **a** corresponds to a flux-weighted Maxwell-Boltzmann distribution defined in Eq. 2 with  $T_{\text{trans}} = 600$  K for 193 nm and 635 K for 351 nm; **b** with  $T_{\text{trans}} = 85$  K. The inset shows a REMPI-TOF spectrum of  $\text{NO}(v = 3)$  at 193 nm, which exclusively consists of component **a**. In the photodissociation at 351 nm,  $\text{NO}(v = 3)$  was not produced. Substrate temperature  $T = 85$  K and chamber pressure  $P = 5 \times 10^{-8}$  Torr.

vibrational excitation of  $\text{NO}(v \leq 9)$  was reported in the 248 nm photodissociation of  $\text{N}_2\text{O}_4$  on LiF(001) by Dixon-Warren et al.<sup>1</sup> In our experiment,  $\text{NO}(v = 3)$  was successfully probed at 193 and 248 nm, but not at 351 nm because the photon energy at 351 nm is too low to produce vibrationally excited  $\text{NO}(v)$ .

A very slow TOF component ( $T_{\text{trans}} = 10 - 30$  K) for  $\text{NO}(v = 0)$  appeared after  $t = 30 \mu\text{s}$  with a relatively small contribution (about one tenth of the total intensity). Actually this slowest component was not observed in a TOF spectrum of vibrationally excited  $\text{NO}(v = 3)$ . This component is considered to be due to false signals caused by  $\text{NO}(v = 0)$  photofragments that are scattered once and bounced back to the REMPI detection region. Hence, the slowest component with  $T_{\text{trans}} = 10 - 30$  K is subtracted from the TOF spectrum of  $\text{NO}(v = 0)$ .

Figure 3 shows typical TOF spectra of  $\text{NO}(v = 0)$  at various substrate temperatures. The experimental conditions were as follows: substrate temperature  $T = 80 - 140$  K, chamber pressure  $P = 50 \times 10^{-8}$  Torr, and dissociation wavelength  $\lambda = 193$

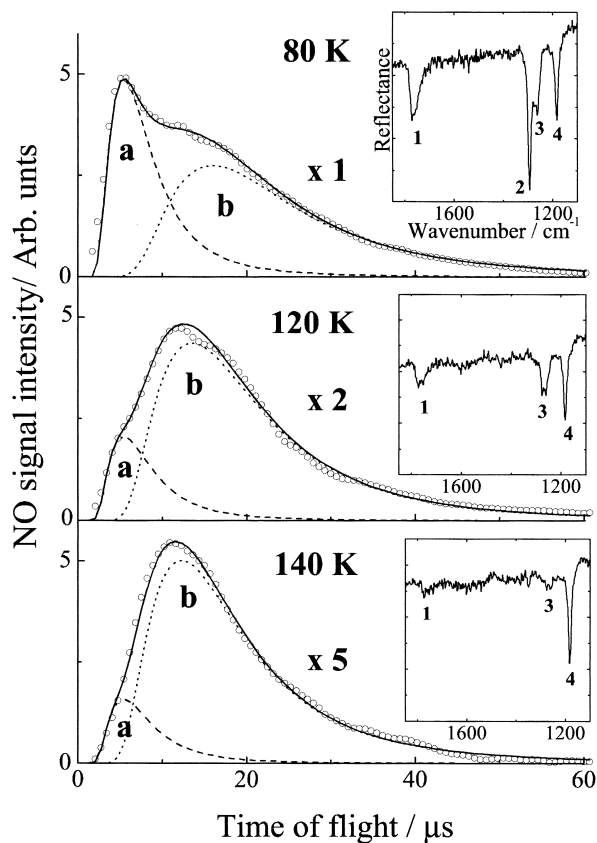


Fig. 3. REMPI-TOF spectra for  $NO(X^2\Pi_{3/2}, v=0, Q\text{-head})$  from the 193 nm photodissociation of  $N_2O_4$  on a polycrystalline Au substrate. Temperatures  $T$  shown in the figure are for the Au substrate. Chamber pressure  $P = 50 \times 10^{-8}$  Torr. Curves correspond to Maxwell-Boltzmann energy distributions with component **a**  $T_{trans} = 740 \pm 20$  K for  $T = 80\text{--}100$  K and  $T_{trans} = 620 \pm 20$  K for  $T = 110\text{--}150$  K, and with component **b**  $T_{trans} = 90 \pm 5$  K for  $T = 80$  K,  $T_{trans} = 105 \pm 5$  K for  $T = 120$  K and  $T_{trans} = 120 \pm 5$  K for  $T = 140$  K. The inset IR spectra show adsorption states of  $N_2O_4$  at various substrate temperatures. Peak 1 is assigned to surface  $N_2O_4$  that adsorbs directly on Au surface and aligns its N-N axis parallel to the surface, peak 2 to multilayer  $N_2O_4$  aligned its N-N axis perpendicular to the surface, peak 3 to random configuration of the surface  $N_2O_4$ , and peak 4 to  $NO_2$  chemisorbed to Au.

nm. Absolute signal intensity decreased with increasing substrate temperature. Comparing the 80 K spectrum in Fig. 3 with the upper panel of Fig. 2, we see that the contribution of component **b** is large (60%) because the film thickness is larger for Fig. 3 than for Fig. 2 ( $P = 5 \times 10^{-8}$  Torr). In Fig. 3, the translational temperatures  $T_{trans}$  for component **b** increases with substrate temperature  $T$ , that is,  $T_{trans} = 90$  K for  $T = 80$  K and  $T_{trans} = 120$  K for  $T = 140$  K. The relative contributions of component **b** increase with substrate temperature  $T$ , reflecting the difference in adsorption states of  $N_2O_4$  at the higher temperature.

The IR spectra in the insets reflect the adsorption states of  $N_2O_4$  at various substrate temperatures. Peak 1 at  $1761\text{ cm}^{-1}$  is assigned to the ONO asymmetric stretching of surface  $N_2O_4$  adsorbed directly on Au surface with its N-N axis aligned par-

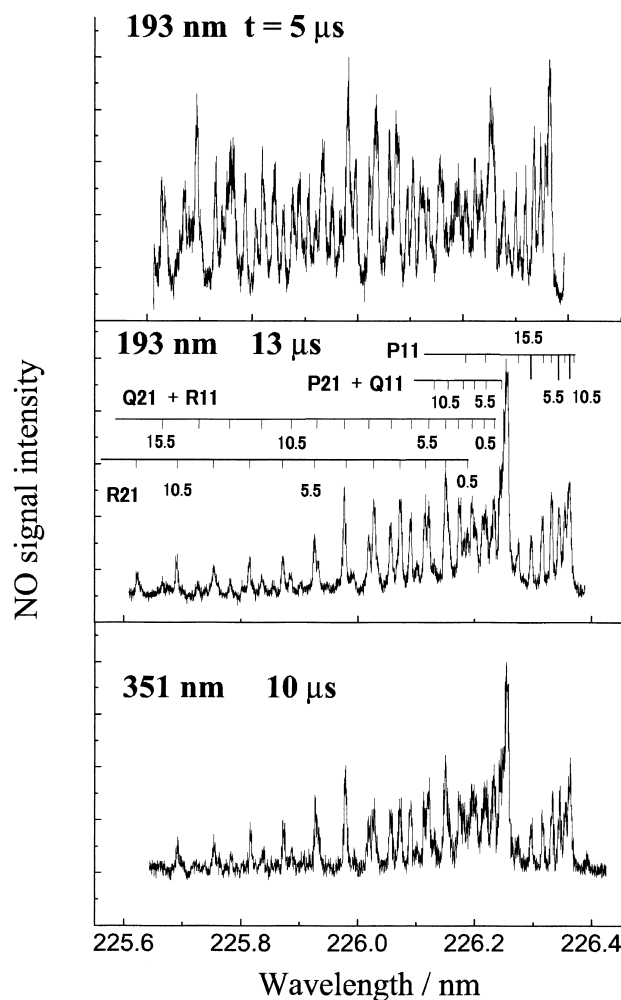


Fig. 4. Rotational spectra of  $NO(A-X, 0-0)$  at different TOF positions,  $t = 5$  and  $13\ \mu\text{s}$ , for the 193 nm photolysis, and at  $10\ \mu\text{s}$  for 351 nm.  $T = 85$  K and  $P = 5 \times 10^{-8}$  Torr.

allel to the surface, peak 2 at  $1296\text{ cm}^{-1}$  to the ONO symmetric stretching of multilayer  $N_2O_4$  with its N-N axis aligned perpendicular to the surface, peak 3 at  $1257\text{ cm}^{-1}$  to random configuration of surface  $N_2O_4$  adsorbed directly on Au surface, and peak 4 at  $1182\text{ cm}^{-1}$  to  $NO_2$  chemisorbed to Au.<sup>4-7</sup> According to a temperature-programmed desorption study by Sato et al.,<sup>4</sup> multilayer  $N_2O_4$  desorbs at 132 K. Thus, the IR intensity of condensed  $N_2O_4$  decreased drastically at 140 K. It may be concluded that the NO signals at 140 K come from the photodissociation of the surface  $N_2O_4$ . These adsorption states will be discussed in Section B of Discussion.

**B. Rotational Spectra of Photofragment NO.** Figure 4 shows the rotational spectra of  $NO(X, v=0, J)$  that was probed for the transition ( $A^2\Sigma, v'=0, J' - X^2\Pi_{3/2}, v''=0, J''$ ) at two different TOF positions,  $t = 5$  and  $13\ \mu\text{s}$  for the 193 nm photolysis, and  $t = 10\ \mu\text{s}$  for 351 nm. The top spectrum of Fig. 4 shows a hot rotational band of NO from the photodissociation at 193 nm and  $t = 5\ \mu\text{s}$ . The spectrum is congested in the R-band region, because the transition due to  $NO(X^2\Pi_{1/2}, v''=0, P\text{-branch})$  overlaps that due to  $NO(X^2\Pi_{3/2}, v''=0, R\text{-branch})$ . The middle panel of Fig. 4 shows a rather cold spectrum observed at  $t = 13\ \mu\text{s}$ . By simulating the spectra for the

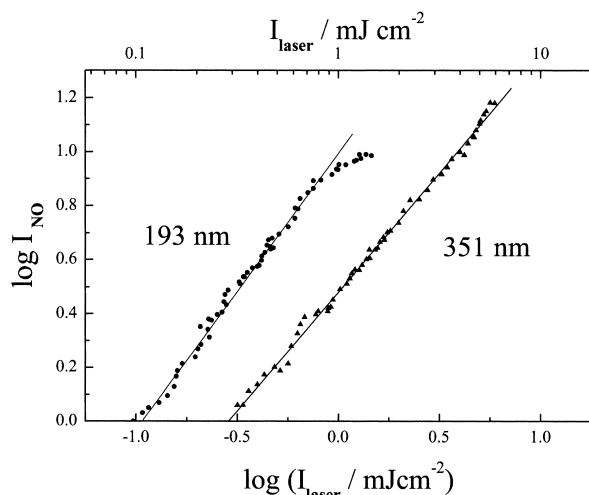


Fig. 5. Signal intensity dependence of NO(X,  $v = 0$ , Q-head) on dissociation laser intensity,  $I_{\text{laser}}$ . The unit slopes shown by the solid lines are suggestive of one-photon dissociation pathways in these laser intensities.  $T = 85$  K and  $P = 5 \times 10^{-8}$  Torr.

non-overlap region, we can estimate rotational temperatures for  $t = 5$  and  $13 \mu\text{s}$  to be  $T_{\text{rot}} = 600$  and  $80$  K, respectively. At  $351$  nm and  $t = 10 \mu\text{s}$ ,  $T_{\text{rot}}$  is  $200$  K. Obviously, the faster photofragment has the higher rotational temperature. The corresponding translational temperatures may be approximated from time-of-flight ( $t$ ) and a fixed flight length  $r$ , using  $2k_{\text{B}}T_{\text{trans}}(t) = (1/2)m(r/t)^2$ ;  $T_{\text{trans}} = 1400$  K ( $5 \mu\text{s}$ ),  $270$  K ( $10 \mu\text{s}$ ) and  $150$  K ( $13 \mu\text{s}$ ). Hasselbrink et al.<sup>2</sup> reported a positive linear correlation between the translational temperatures and rotational energies of the NO fragments from the  $193$  nm photodissociation of the adsorbed  $\text{N}_2\text{O}_4$ . Their results could be described approximately by  $T_{\text{trans}}(\text{K}) = 0.35T_{\text{rot}}(\text{K}) + 700$ . Our results are approximated by a similar equation,  $T_{\text{trans}} = 0.53T_{\text{rot}}$ .

**C. Power Dependence of NO Signal Intensity.** In order to be sure of the number of photons involved in the photoexcitation processes, the laser power dependence for the NO( $v = 0$ ) signal intensity was measured up to  $1 \text{ mJ cm}^{-2}$  at  $193$  nm and to  $5 \text{ mJ cm}^{-2}$  at  $351$  nm. As shown in Fig. 5, the power dependence of the signal intensity was unity, suggestive of a one-photon process for the photodissociation. Typical laser intensities used in the present experiment were  $1 \text{ mJ cm}^{-2}$  at  $193$  nm and  $5 \text{ mJ cm}^{-2}$  at  $351$  nm. Both laser intensities satisfy the condition of one-photon dissociation.

Comparison of the two lines gives relative desorption yield  $\phi(\lambda)$  of NO( $v = 0$ ) at  $193$  and  $351$  nm,  $\phi(351 \text{ nm})/\phi(193 \text{ nm}) = 0.34$ . It is interesting to note that the relative absorption cross section of  $\text{N}_2\text{O}_4$  in the gas phase is  $\sigma_{\text{gas}}(351 \text{ nm})/\sigma_{\text{gas}}(193 \text{ nm}) = 0.013$ .<sup>17</sup> The relative absorption coefficient of Au metal is  $\sigma_{\text{Au}}(351 \text{ nm})/\sigma_{\text{Au}}(193 \text{ nm}) = 0.82$ , which is calculated from the reflection coefficients of Au at the incident angle of  $\pi/4$ .

**D. Effect of  $\text{N}_2\text{O}_4$  Coverage on Time-of-Flight Spectra.** TOF spectra of NO( $v = 0$ , Q-head) were measured for various chamber pressures,  $P = 1\text{--}10 \times 10^{-8}$  Torr and  $T = 85$  K. Figure 6 shows the spectra for  $193$  and  $351$  nm. At  $193$  nm, the fast component **a** is dominant even at the higher pressures.

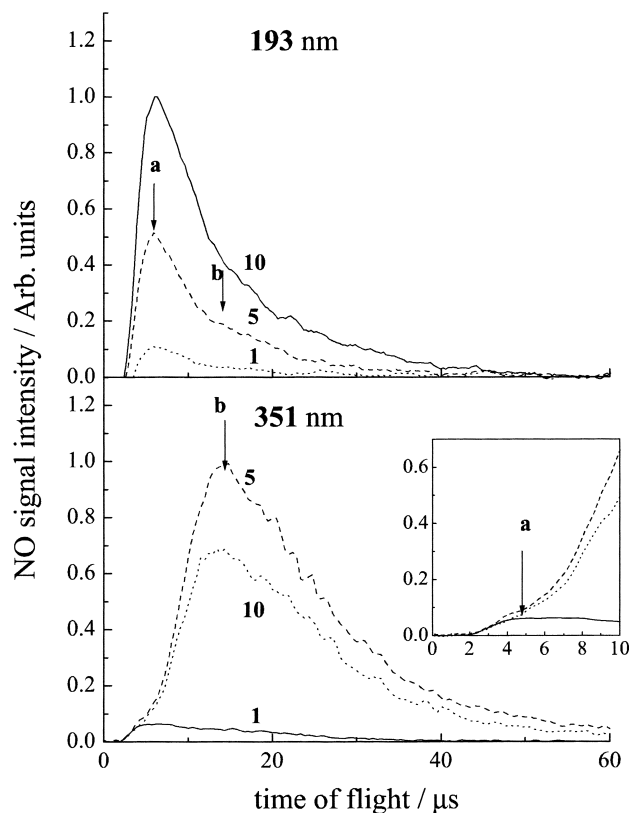


Fig. 6. Effect of chamber pressure,  $P$ , on time-of-flight spectra of NO( $v = 0$ , Q-head) from the photodissociation of  $\text{N}_2\text{O}_4$  on Au at  $193$  and  $351$  nm. The numbers indicated are the chamber pressures in units of  $10^{-8}$  Torr. The arrows marked with **a** and **b** show the peak positions of the fast and slow Maxwell-Boltzmann distributions in Fig. 2. The inset shows an expanded area near the origin.  $T = 85$  K.

However, at  $351$  nm the TOF shape changes drastically as a function of pressure. The fast component **a** is dominant for  $P = 1 \times 10^{-8}$  Torr, while the slow component **b** becomes dominant for  $P = 5\text{--}10 \times 10^{-8}$  Torr ( $1 \text{ Torr} \approx 133.322 \text{ Pa}$ ). The absolute signal intensity initially increases as the pressure increases up to  $P = 5 \times 10^{-8}$  Torr, and then starts decreasing.

The effect of  $\text{N}_2\text{O}_4$  coverage on the signal intensity is shown quantitatively in Fig. 7. At  $193$  nm the slope for component **a** is unity. When the same data were plotted in linear scale, we found that the relation was linear. At  $351$  nm, the intensity of component **b** increases initially, and then decreases at  $P > 5 \times 10^{-8}$  Torr. A similar behavior was observed in the  $248$  nm photodissociation of  $\text{CH}_3\text{Br}$  on brominated Ni(111) by Marsh et al.<sup>6</sup> They reported that the surface mediated slow signal starts decreasing at  $4 \text{ ML}$  region due to collisional quenching, but the fast signal that comes from the photodissociation of top layers increases linearly up to  $10 \text{ ML}$ .

**E. Dependence of Signal Intensity on Polarization of the Incident Light.** Using a pile-of-plates polarizer, the excimer laser light was linearly polarized and the laser intensity was  $0.7 \text{ mJ cm}^{-2}$ . The measured degree of polarization  $\rho$  for the dissociation laser was  $0.71$  at  $193$  nm and  $0.88$  at  $351$  nm. We examined the polarization dependent desorption yields of NO( $v$

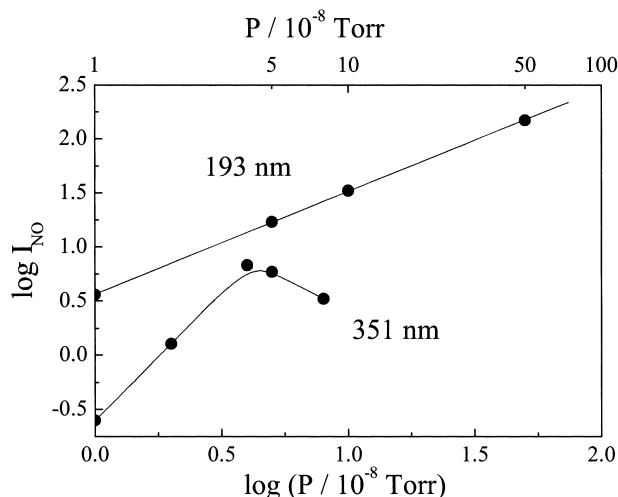


Fig. 7. Signal intensities of NO( $v = 0$ , Q-head) versus reaction chamber pressure,  $P$ . Solid curves are for eye clarity. Signal intensities of NO are measured for component **a** of Fig. 6 at 193 nm and for component **b** at 351 nm.  $T = 85$  K.

= 0) by changing the direction of the electric vector of the incident laser light from parallel (p-polarization) to perpendicular (s-polarization) with respect to the plane of incidence. In our experiment, the angle of incidence  $\phi$  was fixed at  $\pi/4$ . At 80–120 K and for  $P = 2\text{--}5 \times 10^{-8}$  Torr, the signal intensity ratios of  $I_s/I_p$  were measured. After correction for incomplete polarization of the polarized excimer laser light, the ratios were found to be temperature-independent:  $0.88 \pm 0.05$  for the fast component **a** at 193 nm and  $0.65 \pm 0.03$  for the slow component **b** at 351 nm.

As a test, N<sub>2</sub>O<sub>4</sub> was deposited on an amorphous water ice film and was irradiated at 193 nm. The ratio,  $I_s/I_p$ , was unity because randomly oriented N<sub>2</sub>O<sub>4</sub> on the amorphous ice surface absorbs the 193 nm photon. Since electron transfer from a

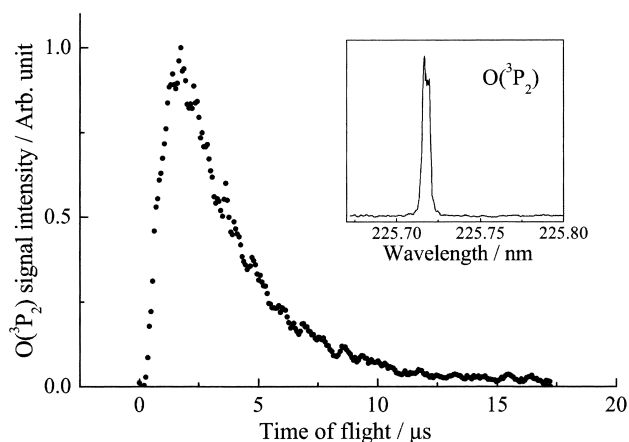


Fig. 8. REMPI TOF spectrum of O(<sup>3</sup>P<sub>2</sub>) from the 193 nm photodissociation of N<sub>2</sub>O<sub>4</sub> on Au. The inset shows the REMPI excitation spectrum of O(<sup>3</sup>P<sub>2</sub>), the flat head of which is due to the two different upper  $j'$  levels.  $T = 80$  K and  $P = 5 \times 10^{-8}$  Torr.

metal surface through the water layer is prohibited,<sup>18</sup> it is unlikely that the dissociation takes place via the surface mediated processes.

**F. Formation of O(<sup>3</sup>P) Atoms.** Two-photon REMPI signals of O(<sup>3</sup>P<sub>*j*</sub>,  $j = 2, 1, 0$ ) atoms were detected from the N<sub>2</sub>O<sub>4</sub> photodissociation at 193 nm. The  $j = 2$  level is most populated, as shown in Fig. 8. Similarly, at 248 nm O(<sup>3</sup>P<sub>*j*</sub>) atoms were detected, but not at 351 nm. The TOF spectrum shown in Fig. 8 consists mainly of the fast component that comes from the photodissociation of the topmost layer of N<sub>2</sub>O<sub>4</sub>. These results are consistent with the fact that the oxygen atoms produced in the layer remain trapped on the Au surface as reported by Sato et al.<sup>4</sup> and Wang et al.<sup>19</sup> The trapped oxygen atoms appear as surface oxygen molecules in their temperature programmed desorption spectra. Since photodissociation takes place on the Au surface at 351 nm, oxygen atoms cannot reach the gas phase from the bottom of the layers.

## Discussion

### A. Photodissociation Primary Processes of N<sub>2</sub>O<sub>4</sub> on Au.

**A-1. Photodissociation at 351 nm.** The following channels are plausible primary processes from an energetic point of view. The energetics is calculated from the gas-phase thermodynamic values:

	$\Delta H(\text{kJ mol}^{-1})$	$\lambda_{\text{threshold}}(\text{nm})$	
N <sub>2</sub> O <sub>4</sub> → NO <sub>2</sub> + NO + O	368	325	(3)
NO <sub>3</sub> + NO	155	430	(4)
N <sub>2</sub> O <sub>3</sub> + O	322	370	(5)

The photon energy of 351 nm is below the thermodynamic threshold for the formation of NO<sub>2</sub> + NO + O. However, Hasselbrink et al.<sup>2</sup> reported the formation of NO from N<sub>2</sub>O<sub>4</sub> on Pd(111) at 351 nm by the laser-induced fluorescence method. Sato et al.<sup>4</sup> reported the formation of O and NO from N<sub>2</sub>O<sub>4</sub> adsorbed on Au(111) at 250–420 nm. One sees the suppression of the NO formation with N<sub>2</sub>O<sub>4</sub> coverage at  $T = 85$  K in Figs. 6 and 7. The inset of Fig. 6 shows that the fast component **a** appears mainly (70%) in the TOF spectrum for the lower coverage or  $P = 1 \times 10^{-8}$  Torr. As the coverage is increased at  $P = 5 \times 10^{-8}$  Torr, the slow component **b** becomes dominant (90%). Further increase of the coverage at  $P = 10 \times 10^{-8}$  Torr leads to a decrease of the signal intensity (Fig. 7). The suppression for the high coverage region indicates that only the photo-products from the layers near the N<sub>2</sub>O<sub>4</sub>–Au interface are released by the photoirradiation. These results suggest that a) the surface mediated excitation occurs at 351 nm, and b) the monolayer coverage is achieved at  $P \sim 1 \times 10^{-8}$  Torr, while the multilayer is formed in between  $P = 1\text{--}5 \times 10^{-8}$  Torr.

The metal surface-mediated photodissociation processes have been reported for many molecules, e.g., N<sub>2</sub>O<sub>4</sub>/Pd,<sup>2</sup> N<sub>2</sub>O<sub>4</sub>/Au,<sup>4</sup> N<sub>2</sub>O/Pt,<sup>3, 20</sup> CH<sub>3</sub>Br/Pt.<sup>8</sup> When the CH<sub>3</sub> signal intensity was monitored by Marsh et al.<sup>8</sup> as a function of coverage of the thin layer CH<sub>3</sub>Br on Pt, the intensity increased first up to four monolayers (4 ML) and then decreased drastically. Coupled with the fact that the fragment velocity is lower relative to the expected gas-phase velocity, it was concluded that the charge transfer process is dominating the fragmentation at low cover-

age of  $\sim 1$  ML. This slow channel dies off steadily from 4 ML to complete extinction at  $\sim 10$  ML. Sato et al.<sup>4</sup> reported that NO is produced from the photodissociation of  $\text{N}_2\text{O}_4$  on Au(111) at  $\lambda \sim 350$  nm (3.5 eV) and its yield is inhibited by the overlayer ( $> 5$  ML) of  $\text{N}_2\text{O}_4$ . In our case, Fig. 7 shows that the signal inhibition starts at  $P = 5 \times 10^{-8}$  Torr, hence we suggest that the coverage at the typical pressure of  $P = 5 \times 10^{-8}$  Torr is 4 to 5 ML. This estimate was supported by our IRAS measurement, which was conducted in a similar dosing condition with a pulsed nozzle.

Since the work function of Au metal is 5.3 eV and the direct electron transfer cannot be induced by the 351 nm excitation, an enhancement mechanism by electron transfer from the substrate may occur. A large increase in the work function upon  $\text{NO}_2$  adsorption on an Au surface implies significant electron transfer from the substrate to chemisorbed  $\text{NO}_2$ .<sup>5</sup> Successive electron transfer would occur from the chemisorbed  $\text{NO}_2$  to multilayer  $\text{N}_2\text{O}_4$  to form a surface species,  $\text{N}_2\text{O}_4^-$ . Thus, it is reasonable to assume that a similar dissociation mechanism occurs in the present experiment at 351 nm. The electron attachment mechanism is also favored to explain the channel where oxygen atoms remain trapped on the Au surface after the photodissociation.

Concerning other possible pathways for the NO formation, the one-color dissociation process of  $\text{NO}_2$  and  $\text{N}_2\text{O}_4$  in the gas phase by the probe laser pulse could be a candidate. When Rieley et al.<sup>21</sup> investigated the photodissociation of  $\text{N}_2\text{O}_4$  multilayers on water layers/Cu at 355 nm, since the size of the  $\text{H}_2\text{O}$  multilayers was 30 ML, no surface mediated process can occur. The direct photoabsorption process of  $\text{N}_2\text{O}_4$  at 355 nm results in the formation of  $\text{NO}_2$  due to N–N bond scission and no desorption of  $\text{N}_2\text{O}_4$ . They estimated the translational energy of the  $\text{NO}_2$  fragment from the surface is 17 meV or 100 K. If, in the present experiment,  $\text{NO}_2$  desorption were followed by its dissociation process due to the probe laser pulse at 226 nm, the 226 nm one-color dissociation would give the signal of highly internally excited NO and also O. However, in the present experiment, a) the observed NO was internally cold, b)  $\text{O}(^3\text{P}_j)$  was not detected. Hence, in our experiment at 351 nm, we can eliminate the possibility of the 226 nm one-color dissociation process for the NO formation from gas-phase  $\text{NO}_2$ .

About the effect of polarization of the incident laser light, s- and p-polarized light,  $I_s/I_p$  was  $0.65 \pm 0.03$ . This ratio is close to that for Au surface photoabsorption. The ratio  $(1-R_s)/(1-R_p)$  for Au at 351 nm is 0.68, where  $R_s$  and  $R_p$  are the reflection coefficients of the Au substrate. This result is consistent with the surface-mediated mechanism. The other photo-process could occur by the electric field induced on the Au surface. The induced field intensities parallel or perpendicular to the surface are calculated with complex refractive indexes and the angle of incidence,  $\phi$ . Details of electromagnetic theory are given by McIntyre<sup>22</sup> and Richter et al.<sup>23</sup> In our case,  $\phi$  was fixed at  $45^\circ$ . According to Ying and Ho,<sup>24</sup> the microscopic field that the surface adsorbed molecules feel is equivalent to the geometric mean of the macroscopic fields between the vacuum and the substrate sides. So, we used the dielectric constant  $\epsilon_{\text{eff}} = 2.54$  for the calculation. The weak electronic transition of  $\text{N}_2\text{O}_4$  at 351 nm is Y-polarized or  $^1\text{B}_{2u}$  in  $\text{D}_{2h}$ .<sup>25, 26</sup> If the orientation of the N–N axis of the adsorbed molecules is

perpendicular to the surface ( $\theta = 0^\circ$ ),  $I_s/I_p$  is calculated to be 0.718. For the case of random orientation ( $\theta = 54.7^\circ$ ), the ratio is 0.567. Since the experimental value is in between these two calculated values, it would not be possible to distinguish the two excitation processes (microscopic electric field or surface-mediated) solely on the basis of the polarization ratio measurement. Sato et al.<sup>4</sup> reported the large reduction effect of 5 ML water layer in the photodissociation of  $\text{N}_2\text{O}_4$  on Au at 350 nm. If the photodissociation takes place by microscopic electric field, there would be no such effect. Thus, we can conclude that the present photoexcitation process at 351 nm is surface-mediated.

**A-2. Photodissociation at 193 nm.** The photon energies at 193 and 248 nm are well above the threshold energy of the formation of NO and O via processes (3–5). Hasselbrink et al.<sup>2</sup> reported the formation of NO from  $\text{N}_2\text{O}_4$  on Pd(111) at 193 nm by the laser-induced fluorescence method. In our experiment, the effect of the coverage of  $\text{N}_2\text{O}_4$  on the time-of-flight spectrum of NO at  $T = 85$  K is shown in Figs. 6 and 7. The linear increase of the NO signal intensity for 193 nm suggests the photodissociation of the topmost layers. Thus, only a slight shape change of the TOF spectra is seen for the pressure range  $P = 1 - 10 \times 10^{-8}$  Torr in Fig. 6. The fast component **a** comes from the photodissociation of the topmost layers of the multilayered  $\text{N}_2\text{O}_4$ . The slow component **b** comes mostly from the photodissociation of the near-surface  $\text{N}_2\text{O}_4$  on Au and partly from the surface-mediated process. The photofragments **b** are translationally and rotationally relaxed almost to the substrate temperature because they undergo rapid relaxation with the metal substrate and by collision with molecules before they come out to the gas phase from the surface.

Concerning the effect of polarization of the incident laser light, s- and p-polarized light, the ratio  $I_s/I_p$  was  $0.88 \pm 0.05$  at 193 nm. Although this ratio is close to that for surface photoabsorption,  $(1-R_s)/(1-R_p) = 0.75$ , the discussion described above suggests that the dissociation at 193 nm does not occur via the surface-mediated process, but via the direct photoabsorption of  $\text{N}_2\text{O}_4$  with the induced electric field on the Au surface. The strong electronic transition of  $\text{N}_2\text{O}_4$  at 185 nm is theoretically and experimentally attributed to Z-polarization or  $^1\text{B}_1$  in  $\text{D}_{2h}$ .<sup>26–28</sup> Using  $\epsilon_{\text{eff}} = 1.84$ ,  $I_s/I_p$  is theoretically calculated to be zero for the perfectly ordered  $\text{N}_2\text{O}_4$  case ( $\theta = 0^\circ$ ), and 0.564 for the randomly oriented case ( $\theta = 54.7^\circ$ ). The calculated value for the random case seems to be in fair agreement with the experimental result. However, the random orientation is not the case according to the IRAS measurements, that is,  $\text{N}_2\text{O}_4$  layers on Au(111) should be ordered layers with the N–N axis perpendicular to the Au surface. Here is our explanation for this discrepancy between the experimental polarization ratio and the theoretical one for the oriented adlayers. As discussed above, the coverage of  $\text{N}_2\text{O}_4$  under our typical experimental conditions was about four to five monolayers. By the present intermittent dosing regime of  $\text{N}_2\text{O}_4$ , the Au surface was almost *replenished* between the photodissociation laser shots, even for the s-polarized light. Thus, the polarization did not work properly for thin-layered molecules, and hence the ratio became close to unity.

**B. Effect of the Adsorption States of  $\text{N}_2\text{O}_4$  on Dissociation Dynamics at 193 nm.** The adsorption states of  $\text{NO}_2$  on

Au were investigated with various methods.<sup>4-7</sup> At 100 K, NO<sub>2</sub> is adsorbed molecularly to form a Au–O<sub>2</sub> nitrosyl surface–chelate with C<sub>2v</sub> symmetry, which is referred as chemisorbed NO<sub>2</sub>. The saturation coverage of chemisorbed NO<sub>2</sub> is 0.4 ML. After the chemisorbed state is saturated, crystalline N<sub>2</sub>O<sub>4</sub> multilayers are formed at 100 K with large exposures of NO<sub>2</sub>. Crystalline N<sub>2</sub>O<sub>4</sub> multilayers are aligned preferentially with the N–N axis perpendicular to the Au(111) surface. The three different TPD peaks of NO<sub>2</sub> from N<sub>2</sub>O<sub>4</sub> on a single crystalline Au(111) surface at three different temperatures, 206, 152 and 132 K, are attributable to desorption of chemisorbed NO<sub>2</sub>, surface N<sub>2</sub>O<sub>4</sub> adsorbed directly on Au, and multilayer N<sub>2</sub>O<sub>4</sub>, respectively.

According to IRAS measurements, the multilayer N<sub>2</sub>O<sub>4</sub> forms an ordered layer, while the surface N<sub>2</sub>O<sub>4</sub> is randomly oriented on the Au. In Fig. 3, as the substrate temperature  $T$  is increased from 80 to 140 K, the adsorption state of the N<sub>2</sub>O<sub>4</sub> layers changes. Multilayer N<sub>2</sub>O<sub>4</sub> is formed at 80 K, while only the surface N<sub>2</sub>O<sub>4</sub> remains on the surface at ~132 K. In Fig. 3, this change in the adsorption state is seen by the change in the relative contributions of the two different TOF components **a** and **b**. At  $T = 80$  K, most of N<sub>2</sub>O<sub>4</sub> are the multilayer N<sub>2</sub>O<sub>4</sub> that feel weak interaction, giving the fast component **a**. At 140 K, the surface N<sub>2</sub>O<sub>4</sub> on Au absorb a 193 nm photon. Since it feels strong interaction with the Au surface, its photodissociation produces predominantly the slow component **b**. The dominant component **b** at  $T = 120$  K is attributable to the slowed components due to its direct contact with Au and due to collisions before the NO fragments come out to the gas phase.

The lower panel of Fig. 3 shows the TOF spectrum for the surface N<sub>2</sub>O<sub>4</sub> adsorbed on Au, which consists of component **b**. However, the TOF spectrum for  $P = 1 \times 10^{-8}$  Torr and  $T = 85$  K consists mostly of component **a**. Under this experimental condition, the average coverage is estimated to be one ML, based on the pressure. This difference arises from the difference in the adsorption state. When the substrate temperature  $T$  is much lower than the desorption temperature (132 K), the pulse deposition of NO<sub>2</sub> would not form a uniform monolayer on Au due to the short duration of 50 ms between pulse deposition and photolysis laser. Probably a part of the Au surface is covered with a multilayer, the topmost layer of which has a larger photodissociation cross section than the surface N<sub>2</sub>O<sub>4</sub>.

**C. Energy Partition in Translational and Rotational Degrees of Freedom.** The translational temperatures of NO increase linearly with the rotational temperatures, as described in Section B of Results. In order to explain the energy partition, we assume an impulse model for direct photodissociation; that is, the consequence of a strong impulsive force acts between atoms. As shown schematically in Fig. 9, NO molecule is forced to separate from the surface species with  $\mathbf{p}_{\text{NO}}$ , and the resulting torque by separation imparts angular momentum on the NO fragment. Let the c.m. momentum of NO be  $\mathbf{p}_{\text{cm}}$  and the angular momentum of NO be  $\mathbf{j}_{\text{NO}}$ ; then,  $E_t = (\mathbf{p}_{\text{cm}})^2/2(m_{\text{O}} + m_{\text{N}})$ , and  $E_r = (\mathbf{j}_{\text{NO}})^2/2I$ , where  $\mu$  and  $I$  are a reduced mass and a moment of inertia of NO. Using the relationships  $\mathbf{p}_{\text{cm}} = \mathbf{p}_{\text{NO}} \cos \theta$  and  $\mathbf{j}_{\text{NO}} = r_{\text{cm}} \times \mathbf{p}_{\text{NO}}$ , where  $\theta$  is the angle between an molecular axis and  $\mathbf{p}_{\text{NO}}$  as defined in Fig. 9 and  $r_{\text{cm}}$  is the distance between the center-of-mass of NO and the N atom, the following relation is given:

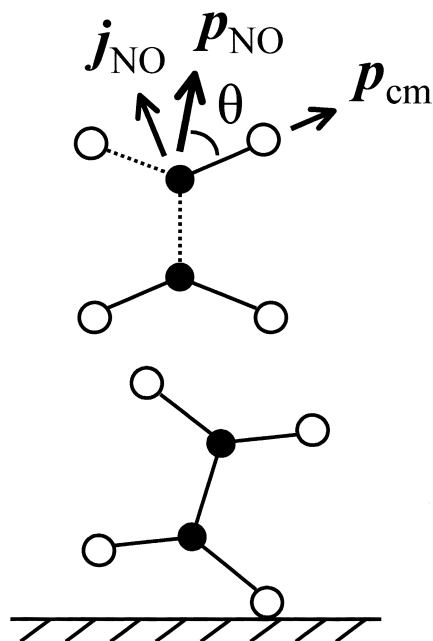


Fig. 9. Schematic diagram of an impulse model for photodissociation of N<sub>2</sub>O<sub>4</sub>.

○: oxygen atom, ●: nitrogen atom,  $\mathbf{p}_{\text{NO}}$ : total momentum of NO fragment produced by separation,  $\mathbf{p}_{\text{cm}}$ : c.m. momentum of NO,  $\mathbf{j}_{\text{NO}}$ : angular momentum of NO.

$$E_{\text{rot}}/E_{\text{trans}} = [m_{\text{O}}m_{\text{N}}/(m_{\text{O}} + m_{\text{N}})]^2 = 0.25. \quad (3)$$

Using  $E_{\text{rot}}/E_{\text{trans}} = T_{\text{rot}}/2T_{\text{trans}}$ , the experimental ratio is 0.23, which is in agreement with the simple momentum conservation rule.

## Conclusion

An N<sub>2</sub>O<sub>4</sub> multilayer (typically 5 ML) adsorbed on polycrystalline Au(111) is photodissociated at  $\lambda = 193$  and 351 nm at 85 K. At 193 nm, the adsorbed N<sub>2</sub>O<sub>4</sub> is directly excited by induced electric field on the Au surface to produce NO and O. The translational energy distribution of NO corresponds to a composite of two Maxwell translational distributions: the fast component of  $T_{\text{trans}} = 600 \pm 30$  K comes from the photodissociation of the top-most layers, the slow component of  $T_{\text{trans}} = 85$ –140 K is attributed to rapid relaxation on the Au surface and also to collisions due to the multilayer dissociation. At 351 nm, the photodissociation process is induced by an enhancement mechanism via electron transfer from the Au substrate. Most of the photofragments are translationally relaxed due to the multilayer dissociation.

The authors thank Prof. Mitsuo Kawasaki for his help in preparation of polycrystalline Au substrates. M.K. thanks the Ministry of Education Science, Sports and Culture for partial support of this work by a Grant-in-Aid for Scientific Research.

## References

- 1 St. J. Dixon-Wallen, R. C. Jackson, J. C. Polanyi, H. Rieley, J. G. Shapter, and H. Weiss, *J. Phys. Chem.*, **96**, 10983 (1992).

- 2 E. Hasselbrink, S. Jakubith, S. Nettesheim, M. Wolf, A. Cassuto, and G. Ertl, *J. Chem. Phys.*, **92**, 3154 (1990).
  - 3 D. P. Masson, E. J. Lanzendorf, and A. C. Kummel, *J. Chem. Phys.*, **102**, 9096 (1995).
  - 4 S. Sato, T. Senga, and M. Kawasaki, *J. Phys. Chem. B*, **103**, 5063 (1999).
  - 5 M. E. Bartram and B. E. Koel, *Surf. Sci.*, **213**, 137 (1989).
  - 6 T. G. Koch, A. B. Horn, M. A. Chesters, M. R. S. McCoustra, and J. R. Sodeau, *J. Phys. Chem.*, **99**, 8362 (1995).
  - 7 J. Wang, B. E. Koel, *J. Phys. Chem. A*, **102**, 8573 (1998).
  - 8 E. P. Marsh, F. L. Tabares, M. R. Scheider, T. L. Gilton, W. Meiser, and J. P. Cowin, *J. Chem. Phys.*, **92**, 2004 (1990).
  - 9 C. C. Johnson and E. T. Jensen, *Surf. Sci.*, **451**, 261 (2000).
  - 10 H. G. Jenniskens, L. Phillipe, M. Kadodwala, A. W. Kleyn, *J. Phys. Chem. B*, **102**, 8736 (1998).
  - 11 M. Kawasaki, *Appl. Surf. Sci.*, **135**, 1159 (1998).
  - 12 S. J. Garret, D. V. Heyd, J. C. Polanyi, *J. Chem. Phys.*, **106**, 7834 (1997).
  - 13 S. J. Garret, D. V. Heyd, J. C. Polanyi, *J. Chem. Phys.*, **106**, 7847 (1997).
  - 14 T-G. Lee, W. Liu, J. C. Polanyi, *Surf. Sci.*, **426**, 173 (1999).
  - 15 J. B. Giorgi, F. Y. Naumkin, J. C. Poanyi, S. A. Raspopov, N. S. -K. Sze, *J. Chem. Phys.*, **112**, 9569 (2000).
  - 16 F. M. Zimmermann and W. Ho, *Surf. Sci. Rep.*, **22**, 127 (1995). In our simulation procedure for the TOF spectra, the following equation  $I(t, r, r_s)$  was used as a signal intensity function, because a) multiphoton-ionization detection of NO is performed at a point that has a flight length  $r$ , hence signal intensity is reduced by a factor of  $r^{-2}$ , and b) the NO photofragments come out to the gas phase from the substrate at a radius  $r_s$ , hence signal intensity is enhanced by a factor of  $2\pi r_s$ :  
$$I(t, r, r_s) = 2\pi S(t, r) r_s r^{-2}.$$
  - 17 A. M. Bass, A. E. Ledford Jr., and A. H. Laufer, *J. Res. Natl. Bur. Stand. Sec. A*, **80**, 143 (1976).
  - 18 T. L. Gilton, C. P. Dehnhostel, and J. P. Cowin, *J. Chem. Phys.*, **91**, 1937 (1989).
  - 19 J. Wang, M. R. Voss, H. Busse, and B. E. Koel, *J. Phys. Chem. B*, **102**, 4693 (1998).
  - 20 J. Kiss, D. Lennon, S. K. Jo, and J. M. White, *J. Phys. Chem.*, **95**, 8054 (1991).
  - 21 H. Rieley, D. J. Colby, D. P. McMurray, and S. M. Reeman, *J. Phys. Chem. B*, **101**, 4982 (1997).
  - 22 J. D. E. McIntyre, *Adv. Electrochem. Eng.*, **9**, 68 (1973).
  - 23 L. J. Richter, S. A. Buntin, D. S. King, and R. R. Cavanagh, *Chem. Phys. Lett.*, **186**, 423 (1991).
  - 24 Z. C. Ying and W. Ho, *J. Chem. Phys.*, **93**, 9089 (1990).
  - 25 W. Niessen, W. Domcke, L. S. Cedarbaum, and J. Schirmer, *J. Chem. Soc. Faraday Trans. 2*, **74**, 1550 (1978).
  - 26 W. N. Sisk, C. E. Miller, and H. S. Johnston, *J. Phys. Chem.*, **97**, 9916 (1993).
  - 27 J. Mason, *J. Chem. Soc., Dalton Trans.*, **1**, 19 (1985).
  - 28 M. Kawasaki, K. Kasatani, H. Sato, H. Shinohara, and N. Nishi, *Chem. Phys.*, **78**, 65 (1983).
-